

# A Hybrid Pressureless Silver Sintering Technology for High-Power Density Electronics

Yuan Zhao,\* Bruno Tolla, Doug Katze, Glenda Castaneda, Jo-Anne Wilson, and David Brand

**Abstract**—Aerospace and defense applications present unique challenges for material suppliers. As increasing adoption of advanced semiconductor materials and Diverse Accessible Heterogeneous Integration technologies, power density of defense and aerospace devices increases rapidly. Traditional die-attaching technology is becoming an increasingly limiting factor in microelectronics packaging for the next generation aerospace and defense systems. Metal particle sintering creates a porous metal foam, which can significantly enhance heat transfer within the sintered material. However, the traditional silver sintering requires very high sintering temperatures that cannot be tolerated by typical microelectronics devices. In addition, the sintered metal foam contains open-cell pores that can absorb/entrap moisture and dusts, which poses a reliability risk. This article introduces an advanced hybrid silver sintering material, which incorporates high-performance silver sintering with high reliability and process-friendly of epoxy-based die-attaching technology. This hybrid sintering paste can be processed without applying any pressures in temperature ranges that are normal in microelectronics packaging processes. Preliminary experimental studies, including Scanning Electron Microscopic study, volume resistivity tests, die shear strength tests, and thermal resistance tests, were performed for developing a low temperature sintering schedule that is compatible with normal assembly processes of high-power density electronics devices. The results indicated that the hybrid material could achieve silver sintering at 150°C and offer  $\times 6$  enhancement on thermal performance comparing with a widely used die-attach material.

**Keywords**—Electronic packaging, thermal management, adhesives, sintering, thermal interface material

## INTRODUCTION

Advancements in multiple technology frontiers, including electronics design, material science, thermal management, and manufacturing technologies, have given birth to wide bandgap (WBG) semiconductors (CS), which are transforming both defense and commercial electronics. For example, Gallium Nitride (GaN)-based high power amplifiers (HPAs) have demonstrated drastically increased breakdown voltage, higher efficiency, and smaller footprint, which leads to exceptional high-power densities. These devices offer broadband performance with higher drain efficiency than Silicon (Si)-based or vacuum electron devices-based solid state power amplifiers. They are increasing replacing Si-based radio frequency (RF) power devices for radar systems. Indium phosphide (InP)-based

material systems have demonstrated high electron mobility and peak velocity, which enables transistors with  $f_{\text{max}}$  exceeding 1 TeraHz [1]. Si carbide (SiC) offers high thermal conductivity and superior high temperature stability, which makes tens of kilowatt-level power switches possible [2]. New compound CS integration platforms initiated by the U.S. Defense Advanced Research Projects Agency (DARPA) through Diverse Accessible Heterogeneous Integration (DAHI) program paved the way for the next generation defense and commercial systems with a goal to achieve integration complexity (number of transistors per circuit) in the order of  $10^{10}$  while maintaining Johnson figure of merit (product of transistor cutoff frequency and breakdown voltage) above  $10^3$  [3]. As more and more transistors are integrated into a single chip, waste heat generated by the chip is increasing rapidly with local heat fluxes approaching several thousand  $\text{W}/\text{cm}^2$  (chip level). It is evident that the advanced high-power density microelectronics devices are becoming more and more thermally limited. New packaging and assembly materials with significantly enhanced thermal performance are highly demanded for the next generation aerospace and defense systems.

Die-attaching technology plays a critical role in packaging and thermal management design for a microelectronics device. The main function of the die attaching is to bond the die onto its substrate/carrier and allow heat to dissipate from heat-generating dice quickly and effectively to ambient. Since the die attach is the closest to the heat source and needs to withstand the most challenging operating conditions (the highest heat flux, the highest temperature, the maximum temperature swings, etc.), it often represents one of the biggest thermal barriers and/or the least liable elements in the entire device. In addition, many advanced high-power electronics devices are vertical in electrical and thermal management design. So, device assembly, especially die-attach in the power devices, need to be both an electrical interconnection and thermal path.

Traditionally, electrically conductive die-attach materials have primarily included solders and electrically conductive die-attaching adhesives. Although solders offer good thermal performance and have been widely used in aerospace applications, their high melting points limit the application processes. Their mechanical stiffness and creep problem poses a long-term reliability risk. Consequently, solders are increasingly being replaced by electrically conductive adhesives (ECAs).

ECA is a curable or thermoset material and typically consists of a polymeric resin, a hardener, and conductive fillers. The curing (or thermosetting) process is a nonreversible process unlike solder reflow, which enables lower process temperature but higher operation temperatures. This process-friendly

The manuscript was received on March 23, 2023; revision received on June 12, 2023; accepted on July 24, 2023.

Henkel Corporation, 14000 Jamboree, Irvine, California 92606

\*Corresponding author; email: yuan-david.zhao@henkel.com

feature not only drastically extends application of the ECAs to new areas beyond traditional solder's territories, but also significantly improves creep resistance at bonding area and thus enhance device reliability.

The polymeric resins typically include epoxy, acrylic, Si, and so on. Epoxy offers excellent mechanical bonding performance and high thermal/chemical stability, which make it a workhorse in the adhesive family. The main weaknesses of the epoxy typically include higher curing temperature and longer curing time. Acrylic offers an alternative solution to offset these weaknesses. Acrylic allows fast curing (snap curing) at lower (or ambient) temperatures for high throughput applications. But its high temperature stability is poor. Si offers excellent high temperature stability as well as improved ability in handling CTE-mismatched assemblies. But its bonding strength is typically orders of magnitude lower than epoxy or acrylic. Epoxy hardener systems include anhydride, imidazole, amine, peroxide, and others.

The most used conductive filler is silver filler (including flakes or spheric particles or mixture of the two). Others include gold, nickel, carbon, silver-plated copper powders, and so on. Traditional technology in making ECAs is to disperse/suspend the conductive fillers in a polymeric resin matrix, which forms point contact between the fillers to conduct electrical current and heat. With this approach, although thermal conductivity of the filler particles is typically as high as several hundred W/mK (i.e., 430 W/mK for silver), the effective thermal conductivity of the ECAs is typically  $<10$  W/mK. There are two reasons for this: (1) The thermal conductivity of the polymer matrix itself is inherently too low (typically around  $.2\text{--}.3$  W/mK). It surrounds and isolates each filler particle and prevents them from effectively transferring heat or electrical current. (2) Since the filler powders are typically very small, multiple particles may be required to fill and bridge a gap between two mating surfaces, which may increase the occurrence of heat transfer interruption by the low conductivity matrix.

To overcome these challenges, many studies have been conducted and multiple new technologies have been developed [4]. The primary objective of these developments centered on replacing the randomly dispensed filler particles with oriented thin wires or platelets with high aspect ratios, such as carbon fibers (CFs), carbon nanotubes (CNTs), graphite nano platelets (GNPs), and copper or silver nanowires. There have been several efforts to grow CNTs directly on substrates as thermal interface materials so that the CNTs are naturally aligned with the heat transfer direction. With this arrangement, Cola et al. realized a thermal resistance of approximately  $.1\text{ cm}^2\text{ K/W}$  under  $.7$  atm pressure [5]. Compared with the  $.09\text{ cm}^2\text{ K/W}$  that can be achieved with conventional solders in the current die-attachment processes [6], this value was still too large. Studies carried out by Kim et al. [7] and Borca-Tasciuc et al. [8] verified this by showing that although individual CNTs have high thermal conductivity, their nanocomposites with polymers have not led to the anticipated large increase in thermal conductivity. The interfacial thermal resistance between the CNT and the host matrix was found to be the main limiting factor that degraded the overall thermal conductivity of the composites. In addition, the quality of CNTs along the growth direction may be poor. For example, if amorphous regions exist, the thermal conductivity of the CNTs is adversely affected. In addition, the in-situ-grown CNT forests are costly and require

high temperature processing that is typically not compatible with microelectronics packaging.

GNPs have also been studied for use as filler powders in polymer systems to improve thermal performance. However, early efforts to use conventional flexible graphite have not yet led to a significant technology breakthrough. Smalc et al. [9] tested several graphite thermal interface materials, developed by mixing exfoliated GNPs with polymeric materials and achieved thermal resistance of  $.9\text{--}1.5\text{ cm}^2\text{ K/W}$  at a thickness of  $130\text{ }\mu\text{m}$  and a pressure of  $100\text{ kPa}$ . Fukushima et al. [10] used exfoliated GNPs as fillers to infiltrate high density polypropylene to form high thermal conductivity nanocomposites and yielded bulk thermal conductivity of  $4\text{ W/mK}$ , which traditional die-attach pastes can easily achieve as well. The Microsystems Technology Office (MTO) of DARPA initiated a series of programs exploring the potential of nanomaterials and nanostructures to create high-performance thermal interface materials. Bar-Cohen et al. [11] conducted a critical review about multiple advanced concepts, including use of metal nanosprings, laminated solder and flexible graphite films, multiwalled CNTs with layered metallic bonding materials, and open-ended CNTs. The advanced research pushed scientific boundaries and showed substantial improvement from the state of the art. Although they were able to achieve thermal interface resistivities well below  $10\text{ mm}^2\text{ K/W}$ , most of these technologies are still in the conceptual stage, and substantial efforts are needed to develop the technology readiness before high volume manufacturing processes can be established.

It is evident that the state-of-the-art filler/resin mixing technologies still have not realized the full potential of the filler materials, nor do they satisfy the thermal cycling requirement in practical applications. The limiting factor is that high conductive fillers are not connected to form a continuous and effective thermal/electrical path.

Realizing the challenges, a new ECA based on hybrid silver sintering-epoxy resin-curing mechanisms has been developed and is presented in this article. The technology is also commonly referred to as semi sintering technology [12].

As previously indicated, the major weakness of traditional ECAs is that fillers are isolated inside a polymer matrix and cannot form an efficient thermal and electrical transport route across the bondline (Fig. 1a), which drastically degrades thermal and electrical performance. Metal particle sintering (i.e., silver sintering), however, can form a well-connected metal structure to effectively transport heat (Fig. 1b). However, the sintered metal structure is typically porous and can absorb and trap moisture due to the large capillary force generated by the small pores. Therefore, in a typical application environment, and especially in aerospace applications, long-term reliability is a serious concern.

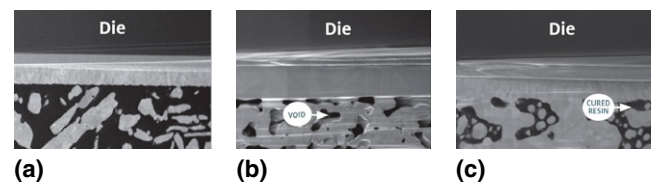


Fig. 1. SEM images of different technologies. (a) Traditional die-attach paste, (b) silver sintering, and (c) Semi sintering.

Alternatively, semi sintering is a hybrid process that marries the advantages of silver sintering with proven resin-curing technologies to create a well-connected metal structure for heat transport. The resin fills and locks all pores to make the entire structure void-free and moisture-resistant (Fig. 1c).

The traditional sintering process typically requires a sintering temperature close to that of the metal melting point, but this temperature cannot be tolerated by typical microelectronics devices. For example, melting point of silver is around  $1,000^{\circ}\text{C}$ , which is significantly beyond tolerance of most microelectronics devices. In defense and aerospace systems, most die-attaching applications prefer process temperature around  $150^{\circ}\text{C}$  or below. So, reducing silver sintering temperature below  $150^{\circ}\text{C}$  is one of the key requirements from the industries.

A novel die-attach adhesive was developed with specially selected and very fine silver particles, which makes low temperature sintering feasible. The semi sintering ECA can be applied via standard stencil or screen printing, dispensing and/or pin transfer, which makes it compatible with most standard assembly processes and equipment.

### EXPERIMENTAL STUDIES

A preliminary study of the semi sintering paste cured at  $200^{\circ}\text{C}$  for 2 h was presented in 2020 [13]. The present work is focused on further lowering the sintering temperature down to  $150^{\circ}\text{C}$  and demonstrating its performance in terms of bond strength, electrical and thermal performance.

Scanning Electron Microscope (SEM) studies were conducted to visually examine/evaluate feasibility of the adhesive sintering at different temperatures. Fig. 2 shows top views of the new adhesive sintered at  $200^{\circ}\text{C}$  for different periods. Fig. 2a shows the SEM image of the adhesive prior to sintering. The silver flakes appeared piled up and aligned horizontally. However, after sintering at  $200^{\circ}\text{C}$  for 2 h, a vastly different structure characteristic from the previous one appeared (Fig. 2b). The silver flakes disappeared, and a porous structure was shown up, which suggested that the silver sintering was achieved. Fig. 2c showed basically a similar porous structure after sintering at  $200^{\circ}\text{C}$  for 6 h, which indicated that Fig. 2b was not a transition state and sintering at  $200^{\circ}\text{C}$  for 2 h was adequate to achieve a silver sintering state. These SEM images were used to establish the benchmark for the subsequent lower temperature sintering studies.

Fig. 3 shows SEM images for sintering at  $150^{\circ}\text{C}$ . Fig. 3a shows the SEM image of the adhesive prior to sintering. The image was similar to Fig. 2a. Fig. 3b shows the state of the adhesive after sintering for 2 h at  $150^{\circ}\text{C}$ . The SEM image was still like Fig. 3a, which suggested that silver fillers were not

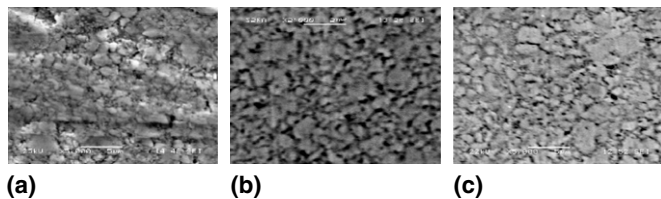


Fig. 2. SEM images of bondline sintered at  $200^{\circ}\text{C}$ . (a) Initial, (b) 2 h, and (c) 6 h.

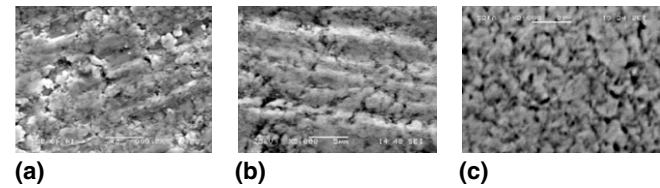


Fig. 3. SEM images at sintering temperature of  $150^{\circ}\text{C}$ . (a) Initial, (b) 2 h, and (c) 6 h.

sintered together yet. However, Fig. 3c showed a porous structure identical to Fig. 2c, which suggested that the silver sintering was achieved.

Combining with Fig. 2, it indicated that the silver sintering could happen after 6 h at  $150^{\circ}\text{C}$  as well as 2 h at  $200^{\circ}\text{C}$ . To verify the SEM findings and demonstrate advantages of semi sintering over traditional ECAs, series of experiments were conducted.

As indicated in previous sections, adhesives based on sintering technology are expected to deliver significantly enhanced electrical and thermal performance over traditional ECAs. Volume resistivity (VR) is a good indicator of electrical conductivity and thus, sintering quality.

Heat transfer in solids is due to the combination of lattice vibrations of the molecules and the energy transport by free flow electrons [14]. In metals, heat conduction occurs mainly by the movement of free electrons inside the metal atoms. This is the reason for why good electric conductors are also good thermal conductors. So, the VR is also a good indicator for heat transfer performance in a silver-sintered structure.

A VR test system was built by using a polycarbonate block (Fig. 4). Four spring-loaded leads were inserted in drilled holes inside the block. The two inner leads with a space of 50 mm are for voltage measurement while the two outer leads provide a DC current to flow through a test sample. An Agilent multimeter (Model 34401A) was used to measure the current and the voltage.

A test specimen was made by coating a 1-mm thick glass slide with a test adhesive (Fig. 5). The coated area had a width of 5 mm and length of 150 mm. Typical coating thicknesses range from 50 to 150 microns. Then, the test specimen was

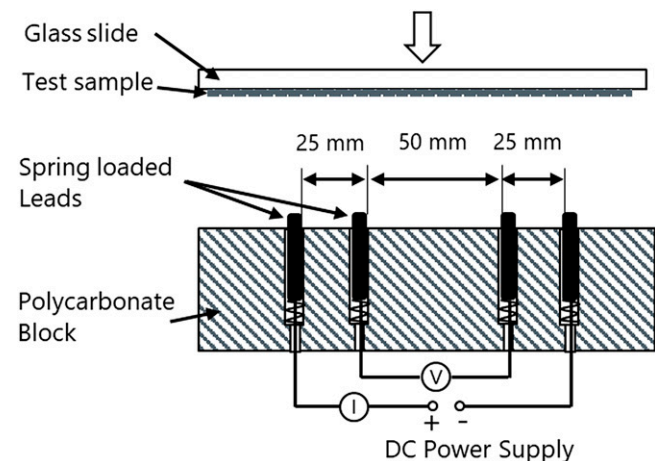


Fig. 4. Schematic of volume resistivity test system.

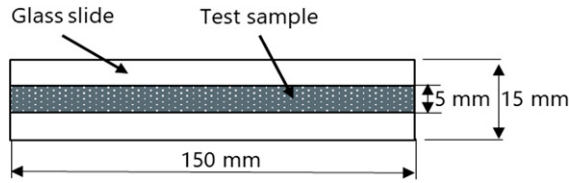


Fig. 5. Schematic of a test specimen (top view of glass slide).

placed in a box oven to cure in accordance with designed curing schedules.

After curing, the test specimen was placed on top of the VR test system with the coated area touching the spring-loaded leads and press them halfway down. Then, current and voltage were recorded. VR of the test ECA is calculated by eq. (1).

$$VR = \frac{V * (w * t)}{I * l} \quad (1)$$

where:

VR = volume resistivity, ohm-cm

V = voltage, V

I = current, A

w = width of the coated section, cm

t = thickness of the coated section, cm

l = length between the two inner leads, cm

Fig. 6 showed VR test results of the new adhesive sintering at 150°C for different periods. VR was around .07 ohm-cm when the ECA sintering for 2 h, which suggests poor or no sintering between particles since traditional ECAs can also achieve this level. However, after sintering for 6 h, the VRs dropped significantly and were below  $2 \times 10^{-5}$  ohm-cm, which approached the VR results of the adhesive sintering at 200°C for more than 2 h (blue area in Fig. 6). This proved that silver sintering was achieved when sintering at 150°C for more than 6 h. These results were consistent with the findings of the SEM study (Fig. 2).

For a die-attach paste, ensuring good and reliable bonding strength is a key requirement. In defense and aerospace systems, copper tungsten (CuW), copper moly (CuM), and kovar are commonly used substrates/carriers for high-power RF devices—primarily because their CTEs are quite close to that of typical CS materials. In this study, CuW thin sheets with a composition of 30% Cu and 70% W were used. The CuW substrates measured 25 mm × 50 mm × 1 mm. Dice used in this

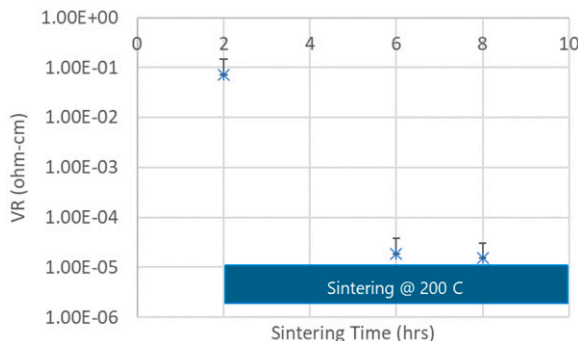


Fig. 6. VR of the new ECA sintering at 150°C.



Fig. 7. Dage 4000 die shear tester.

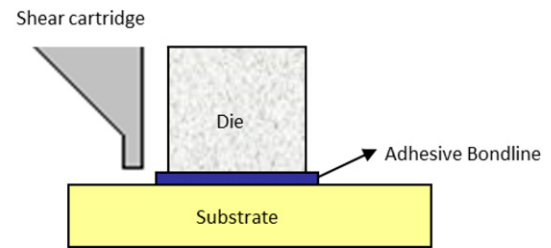


Fig. 8. Schematic of die shear tester.

study were Si dice measuring 2 mm × 2 mm. The CuW substrates were plated with a 1 μm thick silver metallization.

As indicated before, bonding strength of a semi sintered adhesive is provided by combination of cured resin matrix and sintered silver structure. So, bonding strength is expected to increase when silver sintering is achieved. A die shear study was conducted with a Dage 4000 die shear tester (Fig. 7). Schematic of the die shear system is shown in Fig. 8.

Fig. 9 presents die shear test results. It clearly showed that sintering for more than 6 h at 150°C could increase die shear strength significantly, which reinforces the previous conclusions of successfully silver sintering after 6 h at 150°C.

Fig. 10 compared room temperature die shear strength for sintering at 200°C for 2 h and 150°C for 8 h, respectively. The results indicated that the higher sintering temperature schedule

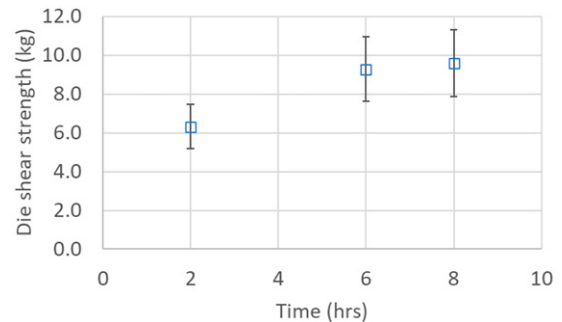


Fig. 9. Room temperature die shear strength of the new ECA sintering at 150°C.



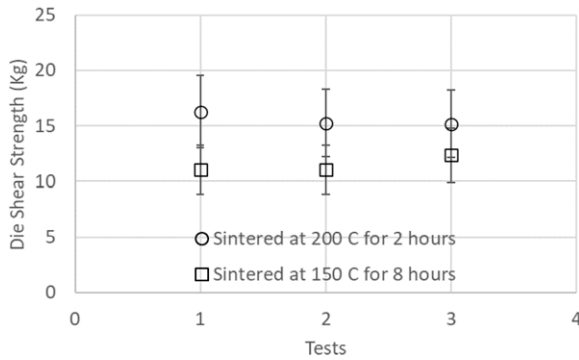


Fig. 10. Die shear strength of the two curing schedules.

achieved approximately 20% higher die shear strength than the 150°C sintering, which might suggest that the higher sintering temperature schedule can achieve a slightly better silver sintering state (more fusion among silver particles) than the lower temperature sintering schedule.

To better understand the sintering schedules and sintering quality, SEM was used to examine cross sectional area of the sintered bondlines. Fig. 11 shows images of sintered silver structures of the two different sintering schedules. Basically, the two SEM images looked similar, which proved that silver sintering was achieved after sintering at 150°C for 8 h. When examining carefully, it appeared that the higher temperature sintering schedule achieved more particle fusion, which created larger “islands” with more interconnections. This can also be used to explain the previous finding that the higher temperature sintering schedule achieved slightly higher bonding strength.

The previous studies successfully demonstrated that the new semi sintering paste could achieve silver sintering at 150°C after sintering for more than 6 h. However, to ensure that the semi sintering adhesive can be used in aerospace applications, proof of high thermal performance in a package is required.

To demonstrate the performance advantages of the semi sintering paste, a widely used die-attach epoxy paste was chosen as control. Key properties of the two pastes are shown in Table I.

Netzsch laser flash LFA 467 equipment was used to evaluate in-package thermal performance of the semi sintering adhesive. The test method was based on trilayer laser flash principles. Gold-plated copper disks with a diameter of 12.7 mm and a thickness of .5 mm were fabricated for building the test specimen (Fig. 12). The test pastes were used to bond a pair of the

Table I  
Key Properties of the Two ECAs

	Control	Semisintering
Technology	Die-attach paste	Semisintering paste
Chemistry	Epoxy	Epoxy
Filler type	Silver	Silver
Volume resistivity (Ohm-cm)	.0005	$2 \times 10^{-5}$
Cure	60 min @ 150°C	6 h at 150°C

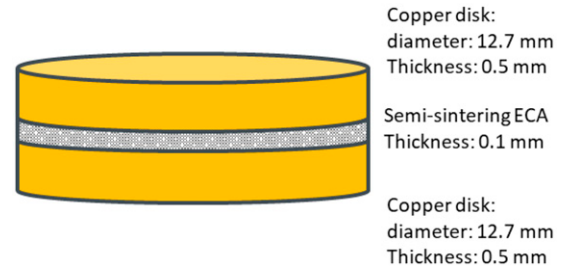


Fig. 12. Trilayer test specimen for laser flash tests.

disks together. And 100  $\mu$ m thick spacers were used during the bonding process to ensure a controllable and uniform bondline thickness.

Upon curing each test specimen, x-ray microscopy was used to examine the bondline and screen test specimen. Fig. 13 shows x-ray images of four test specimens. Among them, one showed significant defects with air entrapment or cracking problems and was removed from the study.

Laser flash tests on the trilayer test specimen were conducted. Effective thermal conductivities and thermal resistances across bondline are shown in Table II. The effective thermal conductivity of the new semi sintering ECA was around 20 W/mK while the control material was around 3.4 W/mK. Thermal resistance of the new semi sintering ECA was approximately .05 Kcm<sup>2</sup>/W while that of the control material was about .3 Kcm<sup>2</sup>/W, which indicates that the new semi sintering ECA offers  $\times 6$  enhancement on thermal performance comparing with the traditional ECA.

Defense and aerospace applications have higher standards in restricting volatile contents inside a material. Outgassing tests were conducted based on ASTM E595-15 standards [15]. The tests were performed in a vacuum environment of  $<5 \times 10^{-5}$  torr for a duration of 24 h at 125°C. Total mass loss (TML), collected volatile condensable materials (CVCML), and amount of water vapor recovered (WVR) were measured and results are shown in Table III. The test results indicated that volatile

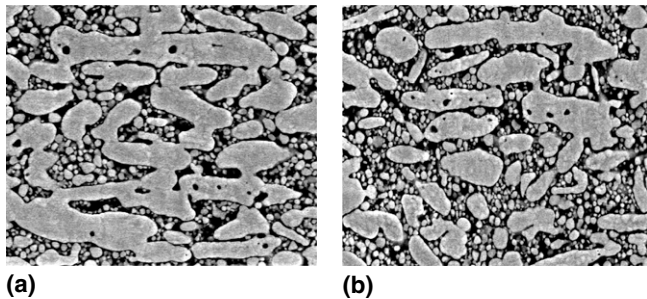


Fig. 11. SEM images of sintered bondlines. (a) Sintering at 200°C for 2 h and (b) sintering at 150°C for 8 h.

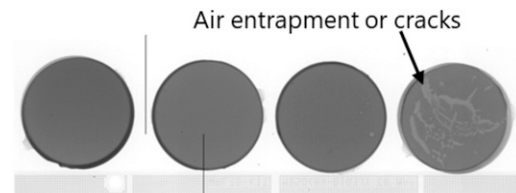


Fig. 13. X-ray images of test specimen sintering at 150°C for 6 h.

Table II  
Thermal Conductivity Test Results

Samples		Effective thermal conductivity (W/mK)	Thermal resistance (Kcm <sup>2</sup> /W)
Control	1	3.3	.3
	2	3.8	.26
	3	3.2	.31
Semisintering	1	18	.056
	2	21	.048
	3	22	.045

Table III  
Outgassing Test Results

	Sintered at 200°C for 2 h	Sintered at 150°C for 8 h
TML	.64%	.81%
CVCM	.09%	.12%
WVR	.03%	.03%

contents were at comparable levels for the two sintering schedules.

## CONCLUSIONS

Comprehensive experimental tests have been conducted to evaluate performances of a new semi sintering ECA. The test results indicated that the new adhesive could achieve silver sintering at 150°C after sintering for 6 h, which meets typical requirements of microelectronics assembly processes. The hybrid silver sintering paste achieved an effective thermal conductivity around 20 W/mK, which significantly outperformed the traditional ECA in thermal performance.

Future work will focus on studying substrate surface metallization or treatment so that the silver sintering can be achieved in a shorter sintering time with enhanced particle-to-surface fusion and heat transfer performance.

## ACKNOWLEDGMENT

The authors would like to thank Dr. Wei Yao for his key contributions in developing the semi sintering ECA.

## REFERENCES

- [1] R. Lai, W.R. Deal, X.B. Mei, W. Yoshida, J. Lee, L. Dang, J. Wang, Y.M. Kim, P.H. Liu, V. Radisic, M. Lange, T. Gaier, L. Samoska, and A. Fung, "Fabrication of InP HEMT devices with extremely high Fmax," The 2008 20<sup>th</sup> International Conference on Indium Phosphide and Related Materials, Versailles, France, 25-29 May 2008.
- [2] B. Ozpineci, M.S. Chinthavali, L.M. Tolbert, A.S. Kashyap, and H.A. Mantooth, "A 55-kW Three-Phase Inverter With Si IGBTs and SiC Schottky Diodes," IEEE Transactions on Industry Applications, Vol. 45, No.1, pp. 278-285, 2009.
- [3] S. Raman, C.L. Dohrman, T.H. Chang, and J.S. Rodgers, "The DARPA Diverse Accessible Heterogeneous Integration (DAHI) program: towards a next-generation technology platform for high-performance microsystems," CS MANTECH Conference, Boston, MA, 23-26 April 2012.
- [4] P. Prasher, "Thermal interface materials: historical perspective, status, and future directions," *Proceedings of the IEEE*, Vol. 94, No. 8, pp. 1571-1586, 2006.
- [5] B. Cola, X. Xu, and T. Fisher, "Increased real contact in thermal interfaces: a carbon nanotube/foil material," *Applied Physics Letters*, Vol. 90, p. 093513, 2007.
- [6] DARPA Broad Agency Announcement, "NanoThermal Interfaces (NTI)," MTO DARPA-BAA-08-42, DARPA Microsystems Technology Office, Arlington, VA, 21 May 2008.
- [7] S. Kim, J. Kim, S. Lee, S. Park, and K. Kang, "Thermophysical properties of multi-walled carbon nanotube-reinforced polypropylene composites," *International Journal of Thermophysics*, Vol. 27, No. 1, pp. 152-160, 2006.
- [8] T. Borca-Tasciuc, M. Mazumder, Y. Son, S.K. Pal, L.S. Schadler, and P.M. Ajayan, "Anisotropic thermal diffusivity characterization of aligned carbon nanotube-polymer composites," *Journal of Nanoscience and Nanotechnology*, Vol. 7, No. 4-5, pp. 1581-1588, 2007.
- [9] M. Smalc, J. Norley, A. Raynolds, III, R. Pachuta, and D.W. Krassowski, "Advanced thermal interface materials using natural graphite," Interpack 2003-35113, Proceedings of IPACK03, International Electronic Packaging Technical Conference and Exhibition, Maui, HI, 6-11 July 2003.
- [10] H. Fukushima, L.T. Drzal, B.P. Rook, and M.J. Rich, "Thermal conductivity of exfoliated graphite nanocomposites," *Journal of Thermal Analysis and Calorimetry*, Vol. 85, No. 1, pp. 235-238, 2006.
- [11] A. Bar-Cohen, K. Matin, and S. Narumanchi, "Nanothermal interface materials: technology review and recent results," *Journal of Electronic Packaging, Transactions of the ASME*, Vol. 137, p. 040803, 2015.
- [12] D. Dixon, "High Thermal, Semi-Sintering Die Attach Paste a Breakthrough for Emerging Package Performance Requirements," <https://www.henkel-adhesives.com/us/en/products/industrial-adhesives/die-attach-adhesives/die-attach-paste.html>.
- [13] Y. Zhao, B. Tollar, D. Katze, G. Castaneda, R. Yoshikawa, and J. Wood, "Hybrid sintering technology for high-power density devices used in aerospace applications," APEX/EXPO IPC 2020, San Diego, CA, 1-6 February 2020.
- [14] T.L. Bergman, A.S. Lavine, F.P. Incropera, and D.P. DeWitt, *Fundamentals of Heat and Mass Transfer*, 8th ed., Wiley, New York, 2017. ISBN: 9781119320425.
- [15] ASTM E595-15, "Standard test method for total mass loss and collected volatile condensable materials from outgassing in a vacuum environment," ASTM International, West Conshohocken, PA, 14 May 2021, [www.astm.org](http://www.astm.org).